

# Cross-Linking Density Effect of Fluorinated Aromatic Polyethers on Transport Properties

Myung-Hwan Jeong, Kwan-Soo Lee, and Jae-Suk Lee\*

Department of Materials Science and Engineering, Gwangju Institute of Science and Technology (GIST), 261 Cheomdan-gwagiro (Oryong-dong), Gwangju 500-712, Korea

Received October 29, 2008; Revised Manuscript Received January 8, 2009

**ABSTRACT:** Novel sulfonated poly(arylene ether) copolymers containing cross-linking moiety and fluorine atoms were prepared for proton exchange membranes of fuel cells. The copolymers were synthesized using potassium 2,5-dihydroxybenzenesulfonate (SHQ), 4,4'-(hexafluoroisopropylidene)diphenol (6F-BPA), decafluorobiphenyl (DFBP), and 1-ethynyl-2,4-difluorobenzene and (CM) as a cross-linking moiety through polycondensation. The chemical structures of the cross-linkable copolymers were analyzed by  $^1\text{H}$  NMR,  $^{19}\text{F}$  NMR, and FTIR-ATR spectra. Cross-linked membranes are obtained by thermal curing of the cross-linkable copolymers. The thermal properties of the cross-linked membranes were characterized by TGA and DSC. Intrinsic viscosity and gel fraction were also evaluated in order to measure the molecular weight and cross-linking density, respectively. The cross-linked network structure greatly suppressed the water uptake and swelling of the cross-linked membrane. The proton conductivity and methanol permeability of the membranes decreased with increasing cross-linking moiety. The decreases in the proton conductivity and methanol permeability are mainly caused by the enhanced barrier properties of the membranes due to the introduction of CM. In other words, the membranes blocked the channels for the passage of water and methanol. The proposed membranes showed moderate proton conductivity and significantly lower methanol permeability when compared to Nafion 212. The SFPE90-CM20 membrane in particular showed low water uptake (37.5%), high proton conductivity (0.091 S/cm), and low methanol permeability ( $37 \times 10^{-8} \text{ cm}^2/\text{s}$ ). The selectivities of all the cross-linked membranes, that is, the ratio of proton conductivity to methanol permeability, fell in the range of  $122 \times 10^3$ – $587 \times 10^3 \text{ S}\cdot\text{s}/\text{cm}^3$ , and they were thus also much higher than the selectivity of Nafion 212 ( $56 \times 10^3 \text{ S}\cdot\text{s}/\text{cm}^3$ ).

## Introduction

A fuel cell is an electrochemical device that converts chemical energy directly into electrical energy by an electrochemical reaction. Fuel cells have become the leading candidates to replace internal combustion engines because of their high power density and environmental friendliness. Among the various types of fuel cells, direct methanol fuel cells (DMFCs) have received much attention for portable power microelectronics applications because they possess several advantages, such as a low operating temperature, easy fuel storage, and low explosive characteristics compared to hydrogen-driven fuel cells.<sup>1,2</sup> However, the commercialization of DMFCs has been hindered by their poor performance, which is due to slow reaction kinetics at the anode, where methanol is oxidized, and methanol crossover through the proton exchange membrane (PEM).

The development of the DMFC has closely followed the improvements of the PEM because the PEM is a key component of fuel cells. Therefore, PEMs have to satisfy several requirements, such as high proton conductivity, low methanol permeability, and sufficient chemical stability. Perfluorosulfonic acid membranes (PFSAs), such as Nafion, the commercially available fluorinated membrane, are commonly used as PEMs because of their excellent chemical resistance and mechanical stability as well as their high proton conductivity. Despite all of these positive features, PFSAs suffer from high cost, low conductivity at high temperatures ( $>100^\circ\text{C}$ ), and high methanol permeability.<sup>3,4</sup> To overcome these problems, many researchers have attempted to find alternative PEMs with low methanol permeability and reasonably high proton conductivity.

Notably, aromatic hydrocarbon polymers have been recognized as some of the most promising candidates, including

poly(ether sulfone)s, poly(ether ketone)s, poly(phenylene)s, polyimides, and polybenzimidazoles, due to their excellent thermal properties, chemical resistance, and mechanical integrity.<sup>5–12</sup> These alternative membranes require a high degree of sulfonation to obtain excellent performance as PEMs. After the addition of sulfonic acid groups, water uptake in the copolymers increases considerably compared to that of the non-sulfonated copolymers. However, the introduction of excess sulfonic acid groups causes excess water uptake, leading to deterioration of the mechanical properties of the membranes. Moreover, the high methanol permeability of membranes is accompanied by high water uptake. For these reasons, the control of water uptake is a very important factor for PEMs.

The introduction of cross-linking moiety into polymer structures is one way to improve PEM properties because it can not only suppress excess water uptake and methanol permeability but also enhance mechanical and chemical stabilities. However, increased cross-linking density reduces proton conductivity and the flexibility of the PEM. Currently, many cross-linking methods have been developed, such as ionic cross-linking and covalent cross-linking.<sup>13–30</sup>

Ionic cross-linking is generally based on interaction forces between different ionomer types, such as acid–base copolymers. PEMs with ionic cross-linking show low water uptake, low methanol permeability, and improved membrane stability. Ionic cross-linking is much more flexible than covalent cross-linking. However, inhomogeneous blend membranes often exhibit poor mechanical stability due to binary blends of immiscible polymers. Another disadvantage of ionic cross-linking is the loss of mechanical strength at temperatures above  $70^\circ\text{C}$ .<sup>13–21</sup> Covalent cross-linking is possible to control water absorption and prevent dissolution of highly sulfonated or water-soluble polymers, thus improving the dimensional stability of the final membranes. In addition, covalently cross-linked membranes

\* To whom correspondence should be addressed: Tel +82-62-970-2306, Fax +82-62-970-2304, e-mail jslee@gist.ac.kr.

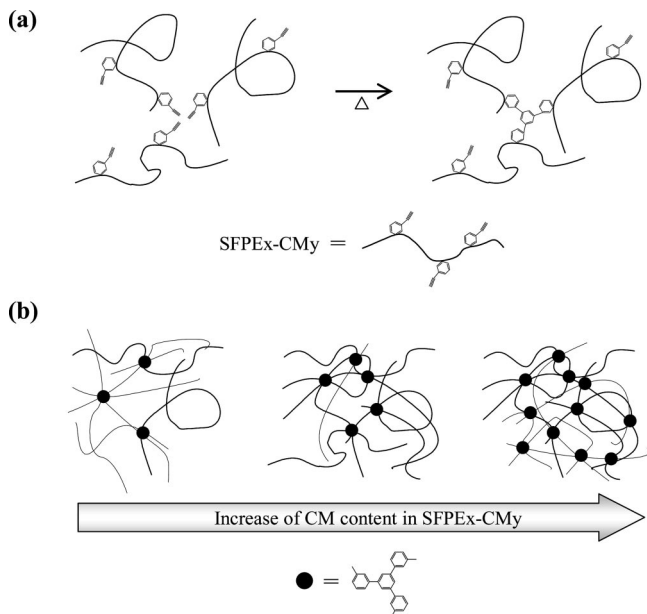


**Figure 1.** Postulated cross-linking mechanism: (a) the cross-linking reaction of ethynyl moiety after thermal curing; (b) the effect of amount of CM in SFPEx-CMy.

have excellent chemical and thermal stability, even at elevated temperatures.<sup>22–30</sup>

The choice of monomers also has a profound influence on the properties of PEMs.<sup>31,32</sup> Monomers containing fluorine atoms offer good chemical resistance and thermo-oxidative stability because the small size and high electronegativity of the fluorine atom confers a strong C–F bond. Moreover, polymers containing fluorinated monomers, such as decafluorobiphenyl, form more hydrophobic structures than non-fluorinated polymers. Thus, these fluorine-containing polymers generally show lower water uptake than their non-fluorinated analogues.

In this study, we report on a new approach for obtaining sulfonated poly(arylene ether) copolymers containing cross-linkable moiety and fluorine atoms. The cross-linkable moiety of the copolymers introduced into the polymer main chain and the regulation of the cross-linking density can easily be controlled by the molar ratio of CM monomer. Cross-linked membranes formed by the cross-linking reaction of ethynyl moiety did not decrease their chemical stability because the ethynyl moiety of the CM monomer formed a benzene ring following thermal curing (Figure 1).<sup>33–35</sup> The cross-linked membranes can achieve high proton conductivity without decreasing ion exchange capacity (IEC) as compared to other covalently cross-linking system.<sup>23,28</sup> Decafluorobiphenyl can be used to increase the hydrophobicity of the membranes for hydrophilic–hydrophobic phase separation. The degree of sulfonation (DS) was controlled by changing the molar ratio of dihydroxy monomers to find the optimum membrane properties.

## Experimental Section

**Materials.** Potassium 2,5-dihydroxybenzenesulfonate (SHQ), 4,4'-(hexafluoroisopropylidene)diphenol (6F-BPA), decafluorobiphenyl (DFBP), 1-ethynyl-2,4-difluorobenzene (CM), benzene, and dimethyl sulfoxide (DMSO) were supplied by Aldrich Chemical Co. Potassium carbonate was dried at 120 °C before use.

**Characterization.** <sup>1</sup>H and <sup>19</sup>F NMR spectra were measured on a JEOL JNM-LA 300 WB FT-NMR in DMSO-*d*<sub>6</sub>. The membranes were analyzed by FTIR-ATR (Jasco 460 Plus, Japan) spectra, with spectra recorded at 4 cm<sup>–1</sup> resolution and measuring 4000–700 cm<sup>–1</sup>. Thermogravimetric analysis (TGA) and differential scanning

calorimetry (DSC) were performed on a TA Instrument 2100 series. Thermal stabilities were determined by TGA in the range of 50–800 °C at a heating rate of 10 °C/min under a nitrogen atmosphere. Glass transition temperatures (*T*<sub>g</sub>'s) were determined by DSC in the range of 50–350 °C at a heating rate of 10 °C/min under a nitrogen atmosphere. Inherent viscosities were determined at a concentration of 0.5 g/dL in DMSO at 25 °C using an Ubbelohde viscometer. The IEC of the cross-linked membranes was measured by classical titration. The dry membranes were soaked in excess of 0.01 M NaCl solution. Released protons were titrated with 0.01 N NaOH solution using phenolphthalein as an indicator.

**Synthesis of Cross-Linkable Copolymers.** The cross-linkable copolymers were prepared from two halide monomers, DFBP and CM, with two hydroxyl monomers, SHQ and 6F-BPA, as shown in Scheme 1. Both DFBP and CM, which was varied to 10–30 mol % based on CM, were reacted with SHQ and 6F-BPA. The molar fraction of SHQ was also varied from 80, 90 to 100% with commercially available monomers. A typical polymerization for all copolymers will be described using the SFPE90-CM10 system.

A 250 mL round-bottom flask was equipped with a Dean–Stark trap, condenser, and nitrogen gas inlet. To the round-bottom flask was added SHQ (5.13 g, 22.5 mmol), 6F-BPA (0.84 g, 2.5 mmol), DMSO (90 mL), benzene (30 mL), and potassium carbonate (4.32 g, 31.25 mmol). The contents of the flask were then heated at reflux for 6 h at 150 °C. After 6 h, water was evaporated as an azeotrope with benzene and was removed in the Dean–Stark trap, and the remaining benzene was distilled from the flask. A solution of DFBP (7.52 g, 22.5 mmol) and CM (0.34 g, 2.5 mmol) in 10 mL of DMSO was added to the flask, and the reaction was stirred for 20 h at 110 °C. The mixture was precipitated into 800 mL of ethanol. The precipitated polymer was filtered and successively washed with deionized water. Drying of the polymer at 60 °C under vacuum gave a brown solid product (yield: 95%).

**Preparation of Membranes.** Membranes were prepared by a solvent-casting methodology. The polymer solutions were prepared from DMSO. The solutions were filtered by using a 0.45 μm Teflon filter and were poured onto a clean glass plate. After casting, the membrane placed on a hot plate with gradual increasing temperature from 50 to 200 °C for 1 h, and the membranes were baked at 250 °C for enough time for the formation of a cross-linking system through the reaction of ethynyl groups.<sup>36–38</sup> The membranes were acidified by immersing in boiling 0.5 M H<sub>2</sub>SO<sub>4</sub> aqueous solution for 2 h, followed by treatment with boiling deionized water for 2 h.<sup>39</sup>

**Measurement of Gel Fraction.** Gel fractions of the networks were measured by solvent extraction.<sup>30,40</sup> An ~0.3 g sample was extracted by Soxhlet extractor using dimethyl sulfoxide (DMSO) as extraction solvent at room temperature. The samples were placed in an excess of DMSO, and the solvent was replaced for 24 h until no further extractable polymer could be detected. The extracted samples were dried until constant weight. The gel fractions were calculated as follows:

$$\text{gel fraction} = \frac{W_2}{W_1} \times 100 (\%) \quad (1)$$

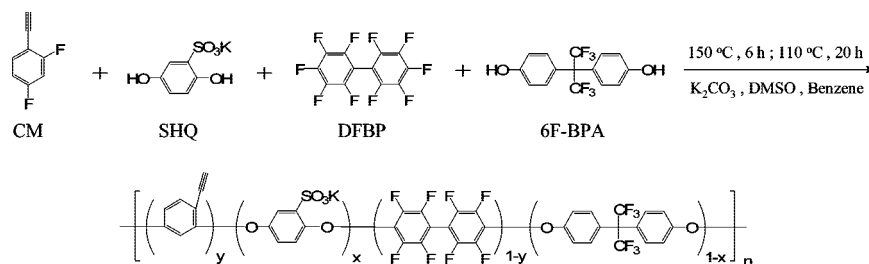
where *W*<sub>1</sub> is the weight of the sample before extraction and *W*<sub>2</sub> is the weight of the dried sample after extraction.

**Proton Conductivity.** Proton conductivity measurement was performed on fully hydrated samples (in water) and was measured using a four-point probe electrochemical impedance analyzer (Solatron 1280Z) over a frequency range from 1 Hz to 1 MHz at room temperature. Using a Bode plot, the frequency region over which the impedance had a constant value was checked, and the resistance was gotten from a Nyquist plot. The proton conductivity was calculated using the following equation:<sup>6,39</sup>

$$\sigma = \frac{L}{RS} \quad (2)$$

where  $\sigma$  (S/cm or Ω<sup>–1</sup> cm<sup>–1</sup>) is proton conductivity, *L* (cm) is the distance between two electrodes, *R* (Ω) is the resistance of

Scheme 1. Synthesis of Cross-Linkable Copolymers (SFPEX-CMy)



membrane, and  $S$  ( $\text{cm}^2$ ) is the surface area of membrane. The impedance of each sample was measured at least five times to ensure data reproducibility.

**Methanol Permeability.** The methanol permeability of the cross-linked membranes was determined using a diffusion cell consisting of two compartments, each compartment containing deionized water (150 mL) and 2 M methanol solution (150 mL). The test membrane was placed between the two compartments, and the diameter of the diffusion area was 1.0 cm. During the test, both compartments were continuously stirred and were maintained at room temperature. Methanol permeates across the membrane by the concentration gradient between the two compartments. The methanol concentration in the deionized water compartment was monitored using a refractive index detector (RI750F, Younglin Instrument Co., Korea) through a 1 mm diameter silicon tube with 1.0 mL/min constant flow driven by a Masterflex pump. The output signal was converted by a data module (Autochro, Younglin Instrument Co., Korea) and recorded by a personal computer. The equation is as follows:<sup>22,39</sup>

$$C_B(t) = \frac{A}{V_B} \frac{DH}{L} C_A(t - t_0) \quad (3)$$

where  $A$  ( $\text{cm}^2$ ) is the effective permeating area,  $V_B$  (mL) is the volume of deionized water compartment,  $D$  ( $\text{cm}^2/\text{s}$ ) is the diffusivity,  $H$  is the partition coefficient,  $L$  (cm) is the thickness of test membrane,  $C_A$  (wt %) is the initial methanol concentration in methanol solution compartment, and  $C_B(t)$  is the methanol concentration in deionized water compartment at diffusion time. The  $DH$  was obtained by extrapolating from the experimentally measured data, with that value considered as the methanol permeability.

## Results and Discussion

**Synthesis and Characterization of SFPEX-CMy.** The synthesis of cross-linkable fluorinated poly(arylene ether) copolymers containing sulfonic acid groups was prepared from an aromatic nucleophilic substitution ( $\text{S}_{\text{N}}\text{Ar}$ ) polycondensation, and the copolymers were prepared with the appropriate molar ratio of potassium 2,5-dihydroxybenzenesulfonate (SHQ) and 4,4'-(hexafluoroisopropylidene)diphenol (6F-BPA) with decafluorobiphenyl (DFBP) and 1-ethynyl-2,4-difluorobenzene (CM) as a cross-linkable moiety. Cross-linkable copolymers are denoted as SFPEX-CMy, where  $x$  is the degree of sulfonation (DS) of the cross-linkable copolymers,  $y$  is the feed ratio of cross-linkable moiety to the total amount of difluoro monomers (mol/mol), and CM is the 1-ethynyl-2,4-difluorobenzene. Scheme 1 outlines a typical procedure for the synthesis of the copolymers.

The cross-linking density can be readily controlled by adjusting the molar ratio of CM monomer, and the monomer was introduced into the polymer main chain. The copolymers also contained varying monomer feed ratios of SHQ (80–100 mol % of total dihydroxy monomer mol %) and CM (10–30 mol % of total dihalide monomer mol %). Both SHQ and 6F-BPA were reacted with DFBP and CM in the presence of potassium carbonate under nitrogen, and DMSO was used as a polymerization solvent. Benzene was also used to remove the

water generated in the activation step of the reaction. All SFPEX-CMy copolymers were obtained under the same polymerization conditions.

The synthesized copolymers were identified by  $^1\text{H}$  NMR and  $^{19}\text{F}$  NMR spectra (Figure 2). The  $^1\text{H}$  NMR spectra of all copolymers contain peaks corresponding to the protons of the cross-linkable moiety in the range of 4.31–4.36, 6.72–6.77, and 7.08–7.15 ppm. Proton peaks due to the SHQ moiety appeared in the range of 7.19–7.38 and 7.47–7.56 ppm. The integration of these proton signals is consistent with the theoretical values. In the  $^{19}\text{F}$  NMR spectra, the ortho and meta positions of fluorine peaks for DFBP are centered at  $-136.25$  and  $-151.70$  ppm, respectively. The disappearance of the para-positioned fluorine atom confirmed the formation of the polymers.

FT-IR spectra were used to analyze the functional groups of the polymer structure. The chemical structures of the cross-linked membranes were confirmed by FTIR-ATR spectra. In Figure 3, the characteristic bands of the aromatic sulfonic acid groups can be observed at  $1023\text{ cm}^{-1}$ . The absorption bands at  $1405\text{ cm}^{-1}$  were assigned to the sulfone ( $\text{O}=\text{S}=\text{O}$ ) of the sulfonic acid groups. The intensity of the two absorption bands increases with DS, which confirms the successful introduction of the sulfonic acid groups into the copolymers. In addition, the IR absorption bands at  $1001\text{ cm}^{-1}$  and around  $1426\text{--}1528\text{ cm}^{-1}$  were characteristic of the  $\text{Ar}-\text{O}-\text{Ar}$  linkage and the aromatic  $\text{C}=\text{C}$  stretching vibration, respectively.

As shown in Table 1, intrinsic viscosities of the cross-linkable copolymers with 10–20 mol % of CM had intrinsic viscosities higher than  $0.98\text{ dL/g}$  in DMSO at  $25\text{ }^\circ\text{C}$ . This indicates that the polymerization successfully produced high molecular weight copolymers. However, other copolymers with CM values above 30 mol % did not yield a high molecular weight due to the relatively low reactivity of CM. All copolymers were soluble in aprotic polar solvents, such as *N*-methylpyrrolidone (NMP), *N,N*-dimethylacetamide (DMAc), and dimethyl sulfoxide (DMSO). This implies that all copolymers were synthesized without side or cross-linking reactions during the polymerization.

**Gel Fractions.** The synthesized cross-linkable copolymers were heated to form a cross-linked network structure after the copolymer solution was poured onto a glass plate. The thermal curing was maintained until the ethynyl moieties of the copolymers reacted. Gel fractions of the cross-linked membranes can be regarded as an indirect method for evaluating the degree of cross-linking.<sup>30,40</sup> Thus, the determination of the gel fraction for the cross-linked membranes is important. The measured gel fractions of the cross-linked membranes are given in Table 1. The gel fractions of the membranes increased with increasing the molar ratio of CM monomer. The results prove that the ethynyl moiety of CM reacted and that the cross-linkable copolymers were cross-linked.

**Thermal Properties.** The thermal stability of the PEM is a key property for the durability during fuel cell operation at high temperature. The thermal stability of the SFPEX-CMy series as



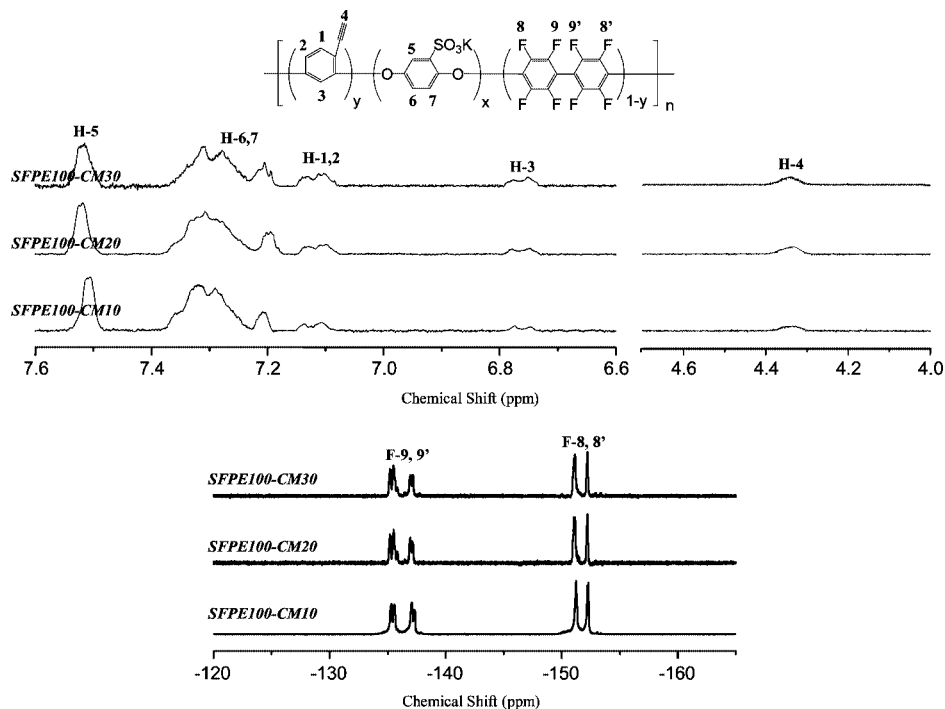


Figure 2.  $^1\text{H}$  NMR and  $^{19}\text{F}$  NMR spectra of SFPE $x$ -CM $y$ .

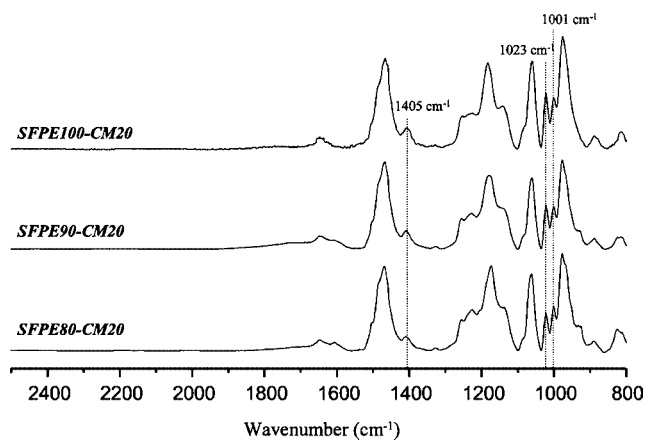


Figure 3. IR spectra of SFPE $x$ -CM $y$ .

Table 1. Inherent Viscosity, Gel Fraction, and Thermal Properties of SFPE $x$ -CM $y$

membrane	feed ratio (mol %) <sup>a</sup>	<i>IV</i> (dL/g) <sup>b</sup>	gel fraction (%) <sup>c</sup>	<i>T</i> <sub>g</sub> (°C) <sup>d</sup>	<i>T</i> <sub>d5%</sub> (°C) <sup>e</sup>
SFPE100-CM10	100/0/10/90	1.48	72.2	257	300
SFPE90-CM10	90/10/10/90	1.32	76.9	249	309
SFPE80-CM10	80/20/10/90	1.18	80.1	236	315
SFPE100-CM20	100/0/20/80	1.26	83.0	291	311
SFPE90-CM20	90/10/20/80	0.98	85.5	280	314
SFPE80-CM20	80/20/20/80	1.03	86.6	264	319
SFPE100-CM30	100/0/30/70	0.75	92.2	312	283
SFPE90-CM30	90/10/30/70	0.83	91.8	296	291
SFPE80-CM30	80/20/30/70	0.90	94.7	278	303

<sup>a</sup> Feed ratios of the monomer SHQ/6F-BPA/CM/DFBP. <sup>b</sup> DMSO at 25 °C. <sup>c</sup> Soxhlet extraction in DMSO for 24 h. <sup>d</sup> Glass transition temperature measured by DSC with a heating rate of 10 °C/min in nitrogen. <sup>e</sup> Onset temperature for 5% weight loss measured by TGA with a heating rate of 10 °C/min in nitrogen.

cross-linked membrane was measured by TGA at a heating rate of 10 °C under a nitrogen atmosphere, and the results are listed in Table 1. All of the cross-linked membranes were dried at 50 °C for several days before thermal analysis. As shown in Figure 4, the cross-linked membranes showed two transitions in weight

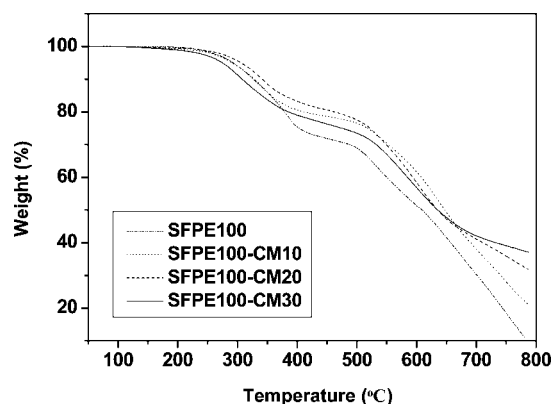


Figure 4. Weight loss of cross-linked membranes and non-cross-linked membrane under nitrogen flow.

loss. The first weight loss step observed in the range of 283–319 °C due to the decomposition of the sulfonic acid groups. The second weight loss step, which was at around 500 °C, is assigned to the decomposition of the polymer main chain. The cross-linked membranes with higher DS degrade more quickly than those with lower DS. As shown in Figure 4, however, the increase of molar ratio in the cross-linkable moiety leads to the increase of the residual char remaining at the final temperature (800 °C). This indicates that the cross-linking of the membranes improves the thermal stability of the polymer main chain.

The membrane with CM form cross-linking network structure for the measurement of TGA and DSC because the reaction of the ethynyl moiety began at around 205 °C.<sup>35,37,38</sup> To show the difference of the thermal stability for non-cross-linked and cross-linked membrane, sulfonated copolymer (SFPE100) without ethynyl moiety was prepared with SHQ and DFBP. In Figure 4, the cross-linked membranes exhibit better thermal stability than the non-cross-linked membrane. The first weight loss step of cross-linked and non-cross-linked membrane is almost the same because of the decomposition of sulfonic acid groups. However, the second weight loss step among them shows a

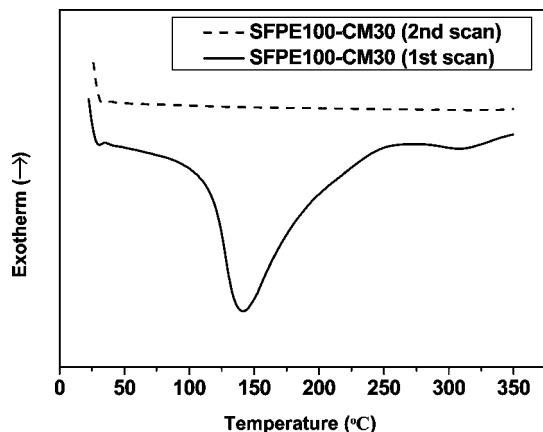


Figure 5. DSC curves of cross-linked membrane.

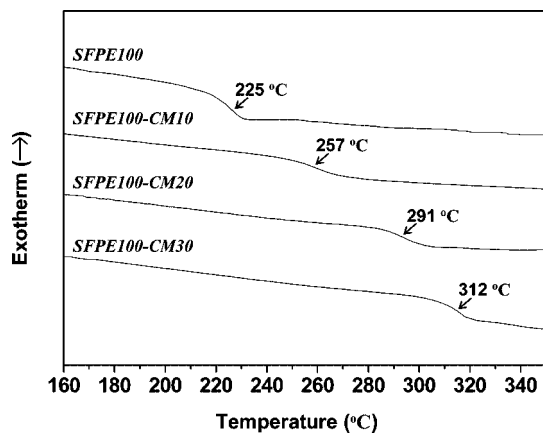


Figure 6. Glass transition temperatures of cross-linked membranes and non-cross-linked membrane under nitrogen flow.

difference because the cross-linking structures improve the thermal stability of the polymer main chain.

In order to evaluate the thermal behavior of the copolymers containing the cross-linking moiety, DSC analysis was performed. The reaction of the ethynyl moiety began at around 205 °C and reached a maximum at about 250 °C.<sup>35,37,38</sup> Thus, the thermal curing of cross-linkable copolymers kept at 250 °C for a sufficient time formed a cross-linked network structure due to the reaction of the ethynyl moiety. In Figure 5, the DSC analysis shows no exothermicity when the cross-linked membranes were first run. This result is supported by a previous report that presented the cross-linking reaction kinetics of ethynyl moieties by DSC.<sup>36–38</sup> The glass transition temperature ( $T_g$ 's) were determined from DSC measurements and are listed in Table 1. Generally, the  $T_g$ 's of sulfonated copolymers increases with increasing DS due to the increase of intermolecular interactions and the molecular bulkiness of the sulfonic acid groups, ranging from 236 to 312 °C, as shown in Table 1.<sup>22,30</sup> The  $T_g$ 's of cross-linked membranes is higher than that of the non-cross-linked membrane, and the  $T_g$ 's of the membranes increased with increasing degree of cross-linking within cross-linked membranes with the same DS, as shown in Figure 6. The improvement of the  $T_g$ 's is contributed to the decreased flexibility of the polymer chains by the formation of cross-linking network structure through the thermal curing.

**IEC, Water Uptake, and Swelling Ratio.** Ion exchange capacity (IEC) is the one of the important factors in the performance of PEMs. Theoretically, IEC increases with DS. SFPE100-CM10 and SFPE100-CM30 have different IEC values, though they have the same DS because they contain the different molar ratio of monomers in the polymer repeating unit. This

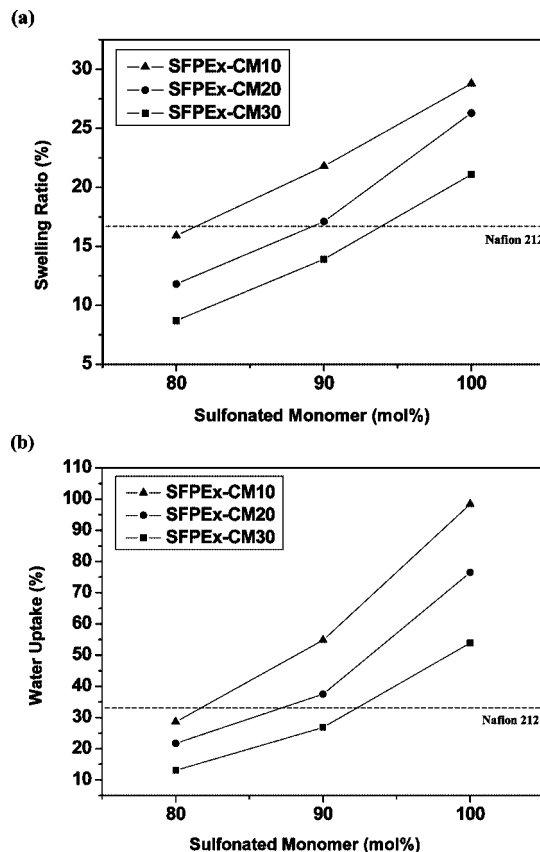


Figure 7. Swelling ratio (a) and water uptake (b) versus the molar ratio of sulfonated monomer. In the SFPE<sub>x</sub>-CM<sub>10</sub>, SFPE<sub>x</sub>-CM<sub>20</sub>, and SFPE<sub>x</sub>-CM<sub>30</sub>,  $x$  is the molar ratio of sulfonated monomer, that is,  $x = 80, 90$ , and  $100$  mol %.

also accounts for the different properties of these membranes. SFPE100-CM10 has a water uptake of 98.4% and a proton conductivity of 0.123 S/cm at an IEC of 2.08 mequiv/g, while SFPE100-CM30 has a water uptake of 53.9% and a proton conductivity of 0.103 S/cm at an IEC of 2.20 mequiv/g.

The water uptake and swelling ratio of the membranes are also important properties for fuel cell operation due to their important effects on the proton conductivity and the methanol permeability as well as the dimensional stability of the membranes. Excess water absorption leads to morphological instability; on the other hand, a lack of water absorption results in low proton conductivity. Consequently, the management of water is an essential factor for optimized fuel cell operation. Figure 7 presents the water uptake and swelling ratios of the cross-linked membranes as a function of the molar ratio of sulfonated monomer. As expected, the water uptake and swelling ratios of the membranes increase with DS because the presence of sulfonic acid groups in the polymer main chain increases the ionic nature of the sulfonated copolymers. However, the water uptake and swelling ratios decrease with increasing molar ratio of CM monomer within the membranes with the same DS (Table 2). It can be concluded that cross-linking is a useful method for constraining the water uptake, since the networks result in smaller hydrophilic channels for water absorption.<sup>15,29,30</sup>

**Proton Conductivity and Methanol Permeability.** Through transport experiments, the proton conductivity and methanol permeability were determined. The proton conductivity of the cross-linked membranes was measured while the membranes were fully hydrated and all of the membranes were soaked in water for hydration before the measurement of methanol permeability was conducted at room temperature. For comparison, the proton conductivity and methanol permeability of

**Table 2. IEC, Water Uptake, Swelling Ratio, Proton Conductivity, and Methanol Permeability of Cross-Linked Membranes**

membrane	IEC (mequiv/g)		water uptake (%) <sup>c</sup>	swelling ratio (%) <sup>d</sup>	proton conductivity (S/cm)	methanol permeability (10 <sup>-8</sup> cm <sup>2</sup> /s)
	calcd IEC <sup>a</sup>	exptl IEC <sup>b</sup>	room temp	room temp	room temp	room temp
SFPE100-CM10	2.15	2.08	98.4	28.8	0.123	101
SFPE90-CM10	1.88	1.84	54.8	21.8	0.106	58
SFPE80-CM10	1.62	1.58	28.6	15.9	0.065	30
SFPE100-CM20	2.25	2.15	76.5	26.3	0.111	71
SFPE90-CM20	1.96	1.91	37.5	17.1	0.091	37
SFPE80-CM20	1.69	1.62	21.7	11.8	0.058	18
SFPE100-CM30	2.35	2.20	53.9	21.1	0.103	52
SFPE90-CM30	2.05	1.96	26.8	13.9	0.080	25
SFPE80-CM30	1.76	1.67	13.1	8.7	0.047	8
Nafion 212	0.95–1.01 <sup>e</sup>	0.97	32.8	16.7	0.093	165

<sup>a</sup> Calculated ionic exchange capacity (IEC). <sup>b</sup> Measured after soaking in 0.01 M NaCl solution for 24 h and then titrated with 0.01 N NaOH solution using phenolphthalein as an indicator at rt. <sup>c</sup> Water uptake (%) =  $\{(W_{\text{wet}} - W_{\text{dry}})/W_{\text{dry}}\} \times 100$ , where  $W_{\text{wet}}$  and  $W_{\text{dry}}$  are the weights of swollen and dried membranes, respectively. <sup>d</sup> Swelling ratio (%) =  $(L_{\text{wet}} - L_{\text{dry}})/L_{\text{dry}} \times 100$ , where  $L_{\text{wet}}$  and  $L_{\text{dry}}$  are the lengths of swollen and dried membranes, respectively. <sup>e</sup> Data obtained from ref 41.

Nafion 212 were measured under the same experimental conditions. In the cross-linked membranes with the same molar ratio of cross-linkable moiety, the proton conductivity and methanol permeability of the membranes increase with DS at room temperature. These results are consistent with the water uptake and swelling ratios (Table 2). This is due to the increase in the number of sulfonic acid groups ( $\text{SO}_3\text{H}$ ), which form the sites for the transport of proton and methanol, and to the increase in water uptake, which plays an important role in increasing the mobility of protons and methanol through the membrane. Some of the cross-linked membranes exhibited higher proton conductivities, exceeding 0.1 S/cm, than that of Nafion 212 at room temperature, while the methanol permeabilities of the membranes were much smaller than that of Nafion 212.

Figure 8 shows the proton conductivity and methanol permeability through the cross-linked membranes as a function of the CM feed ratio. The more cross-linkable moiety is introduced, the lower are the proton conductivity and methanol permeability in the cross-linked membranes with same DS. The results indicate that the proton conductivity and methanol permeability of the cross-linked membranes decrease with increasing cross-linking density because cross-linking reduces the size of the ionic channels, resulting in the suppressed transport of protons and methanol.<sup>15,29,30</sup> Nevertheless, the proton conductivity and methanol permeability of the membranes still had reasonable values. All of the cross-linked membranes showed proton conductivities higher than 0.047 S/cm and methanol permeabilities lower than  $101 \times 10^{-8} \text{ cm}^2/\text{s}$ . In the case of SFPE100-CM30, the proton conductivity and methanol permeability were 0.103 S/cm and  $52 \times 10^{-8} \text{ cm}^2/\text{s}$ , respectively. Accordingly, the introduction of cross-linking moiety was indispensable in obtaining desirable properties for the membranes as proton conductors in fuel cells.

**Selectivity.** Selectivity, which is defined as the ratio of proton conductivity to methanol permeability, is a significant value because the higher the selectivity of the membrane is, the better the membrane can perform as both a good conductor and a good separator in DMFC. The selectivity of the cross-linked membranes as a function of the cross-linking density and DS is shown in Figure 9. The selectivity of cross-linked membranes increases with increasing the molar ratio of cross-linking moiety and with decreasing DS. The cross-linked membranes exhibit selectivities in the range from  $122 \times 10^3$  to  $587 \times 10^3 \text{ S}\cdot\text{s}/\text{cm}^3$ . These are approximately 2–10 times higher than the selectivity of Nafion 212 ( $56 \times 10^3 \text{ S}\cdot\text{s}/\text{cm}^3$ ). Figure 9 demonstrates that control of the cross-linking density makes optimum proton conductivity and methanol permeability possible.

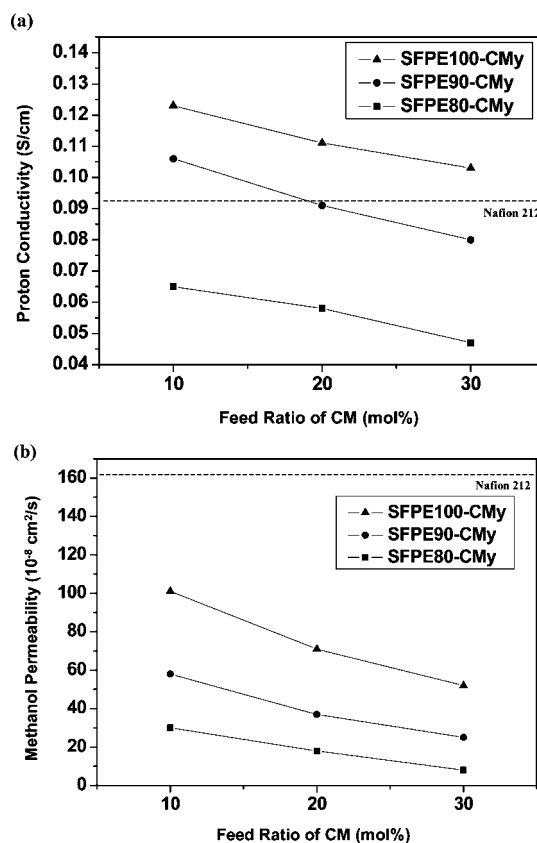


**Figure 8.** Influence of the CM feed ratios on proton conductivity (a) and methanol permeability (b). In the SFPE100-CMy, SFPE90-CMy, and SFPE80-CMy, y is the feed ratio of CM, that is,  $y = 10, 20$ , and  $30 \text{ mol } \%$ .

## Conclusions

New cross-linkable copolymers (SFPE $x$ -CM $y$ ) were successfully synthesized by controlling the feed ratio of SHQ, as the hydrophilic part, and CM, as a cross-linkable moiety. The copolymers incorporated the cross-linkable moiety into the polymer main chain. Cross-linked membranes were prepared by thermal curing, and the membranes formed cross-linked network structures with covalent bonds. Cross-linking greatly reduced the water uptake and the swelling ratio of the membranes, while high proton conductivity and low methanol permeability were maintained. We found that these kinds of transport properties were greatly dependent on the cross-linking density (the molar ratio of CM monomer) and the degree of sulfonation (the molar ratio of SHQ monomer). In our work, most of the cross-linked membranes had proper water uptakes,

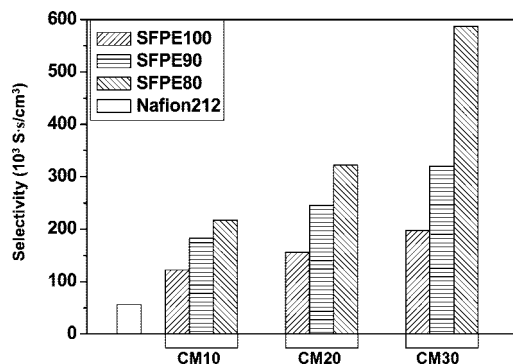


**Figure 9.** Selectivity of cross-linked membranes (selectivity = proton conductivity/methanol permeability).

and all of the cross-linked membranes showed good proton conductivities (0.047–0.123 S/cm) and low methanol permeabilities ( $8 \times 10^{-8}$ – $101 \times 10^{-8}$  cm<sup>2</sup>/s). The SFPE90-CM20 membrane showed the best membrane properties, with a water uptake of 37.5%, a good proton conductivity of 0.091 S/cm, and a low methanol permeability of  $37 \times 10^{-8}$  cm<sup>2</sup>/s. The optimum values can also be attributed to the degree of control for the feed ratio of cross-linkable moiety and DS. In this study, we have proved that cross-linking is as effective as DS in changing the transport properties. These results indicate that the SFPE<sub>x</sub>-CM<sub>y</sub> series of cross-linked membranes is a promising candidate for optimizing the polymer structure of PEMs for fuel cell applications.

**Acknowledgment.** This research was partially supported by a grant (#07 seaHERO B02-03-01) from Plant Technology Advancement Program funded by Ministry of Land, Transport and Maritime Affairs of Korean government.

## References and Notes

- (1) Neburchilov, V.; Martin, J.; Wang, H.; Zhang, J. *J. Power Sources* **2007**, *169*, 221.
- (2) Kamarudin, S. K.; Daud, W. R. W.; Ho, S. L.; Hasran, U. A. *J. Power Sources* **2007**, *163*, 743.
- (3) Souzy, R.; Ameduri, B. *Prog. Polym. Sci.* **2005**, *30*, 644.
- (4) Mauritz, K. A.; Moore, R. B. *Chem. Rev.* **2004**, *104*, 4535.
- (5) Miyatake, K.; Chikashige, Y.; Watanabe, M. *Macromolecules* **2003**, *36*, 9691.
- (6) Wang, F.; Hickner, M.; Ji, Q.; Harrison, W.; Mecham, J.; Zawodzinski, T. A.; McGrath, J. E. *Macromol. Symp.* **2001**, *175*, 387.
- (7) Wang, L.; Meng, Y. Z.; Wang, S. J.; Shang, X. Y.; Li, L.; Hay, A. S. *Macromolecules* **2004**, *37*, 3151.
- (8) Xing, P.; Robertson, G. P.; Guiver, M. D.; Mikhailenko, S. D.; Kaliaguine, S. *Macromolecules* **2004**, *37*, 7960.
- (9) Nakabayashi, K.; Matsumoto, K.; Shibasaki, Y.; Ueda, M. *Polymer* **2007**, *48*, 5878.

- (10) Fang, J.; Guo, X.; Harada, S.; Watari, T.; Tanaka, K.; Kita, H.; Okamoto, K. *Macromolecules* **2002**, *35*, 9022.
- (11) Asano, N.; Aoki, M.; Suzuki, S.; Miyatake, K.; Uchida, H.; Watanabe, M. *J. Am. Chem. Soc.* **2006**, *128*, 1762.
- (12) Xu, H.; Chen, K.; Guo, X.; Fang, J.; Yin, J. *Polymer* **2007**, *48*, 5556.
- (13) Fu, Y.; Manthiram, A.; Guiver, M. D. *Electrochem. Commun.* **2006**, *8*, 1386.
- (14) Yin, Y.; Hayashi, S.; Yamada, O.; Kita, H.; Okamoto, K. *Macromol. Rapid Commun.* **2005**, *26*, 696.
- (15) Zhong, S.; Cui, X.; Cai, H.; Fu, T.; Shao, K.; Na, H. *J. Power Sources* **2007**, *168*, 154.
- (16) Yang, S. J.; Jang, W.; Lee, C.; Shul, Y. G.; Han, H. S. *J. Polym. Sci., Part B: Polym. Phys.* **2005**, *43*, 1455.
- (17) Hofmann, M. A.; Ambler, C. M.; Maher, A. E.; Chalkova, E.; Zhou, X. Y.; Lvov, S. N.; Allcock, H. R. *Macromolecules* **2002**, *35*, 6490.
- (18) Kerres, J.; Ullrich, A.; Meier, F.; Häring, T. *Solid State Ionics* **1999**, *125*, 243.
- (19) Walker, M.; Baumgärtner, K. M.; Kaiser, M.; Kerres, J.; Ullrich, A.; Räuchle, E. *J. Appl. Polym. Sci.* **1999**, *74*, 67.
- (20) Kerres, J. A. *Fuel Cells* **2005**, *5*, 230.
- (21) Deimede, V.; Voyiatzis, G. A.; Kallitsis, J. K.; Qingfeng, L.; Bjerrum, N. J. *Macromolecules* **2000**, *33*, 7609.
- (22) Rhim, J. W.; Park, H. B.; Lee, C. S.; Jun, J. H.; Kim, D. S.; Lee, Y. M. *J. Membr. Sci.* **2004**, *238*, 143.
- (23) Mikhailenko, S. D.; Wang, K.; Kaliaguine, S.; Xing, P.; Robertson, G. P.; Guiver, M. D. *J. Membr. Sci.* **2004**, *233*, 93.
- (24) Zhang, W.; Gogel, V.; Friedrich, K. A.; Kerres, J. *J. Power Sources* **2006**, *155*, 3.
- (25) Li, Q.; Pan, C.; Jensen, J. O.; Noyé, P.; Bjerrum, N. J. *Chem. Mater.* **2007**, *19*, 350.
- (26) Lee, C. H.; Park, H. B.; Chung, Y. S.; Lee, Y. M.; Freeman, B. D. *Macromolecules* **2006**, *39*, 755.
- (27) Heo, K. B.; Lee, H. J.; Kim, H. J.; Kim, B. S.; Lee, S. Y.; Cho, E.; Oh, I. H.; Hong, S. A.; Lim, T. H. *J. Power Sources* **2007**, *172*, 215.
- (28) Zhang, C.; Guo, X.; Fang, J.; Xu, H.; Yuan, M.; Chen, B. *J. Power Sources* **2007**, *170*, 42.
- (29) Zhong, S.; Cui, X.; Cai, H.; Fu, T.; Zhao, C.; Na, H. *J. Power Sources* **2007**, *164*, 65.
- (30) Ding, F. C.; Wang, S. J.; Xiao, M.; Meng, Y. Z. *J. Power Sources* **2007**, *164*, 488.
- (31) Harrison, W. L.; Wang, F.; Mecham, J. B.; Bhanu, V. A.; Hill, M.; Kim, Y. S.; McGrath, J. E. *J. Polym. Sci., Part A: Polym. Chem.* **2003**, *41*, 2264.
- (32) Gao, Y.; Robertson, G. P.; Guiver, M. D.; Mikhailenko, S. D.; Li, X.; Kaliaguine, S. *Polymer* **2006**, *47*, 808.
- (33) Saaby, S.; Baxendale, I. R.; Ley, S. V. *Org. Biomol. Chem.* **2005**, *3*, 3365.
- (34) Saito, S.; Yamamoto, Y. *Chem. Rev.* **2000**, *100*, 2901.
- (35) Lee, K.-S.; Jeong, M.-H.; Lee, J.-P.; Lee, J.-S. *Macromolecules*, DOI: 10.1021/ma802233j.
- (36) Lee, H.-J.; Lee, M.-H.; Oh, M.-C.; Ahn, J.-H.; Han, S. G. *J. Polym. Sci., Part A: Polym. Chem.* **1999**, *37*, 2355.
- (37) Lee, K.-S.; Lee, J.-S. *Chem. Mater.* **2006**, *18*, 4519.
- (38) Kim, J.-P.; Lee, W.-Y.; Kang, J.-W.; Kwon, S.-K.; Kim, J.-J.; Lee, J.-S. *Macromolecules* **2001**, *34*, 7817.
- (39) Kim, Y. S.; Hickner, M. A.; Dong, L.; Pivovar, B. S.; McGrath, J. E. *J. Membr. Sci.* **2004**, *243*, 317.
- (40) Paul, M.; Park, H. B.; Freeman, B. D.; Roy, A.; McGrath, J. E.; Riffle, J. S. *Polymer* **2008**, *49*, 2243.
- (41) From Dupont Material Data sheet at <http://www.fuelcell.com/tech-sheets/Nafion%20NRE-211%20212.pdf>.

MA8024199